delocalization of the Pt($5d_{z^2}$) electrons. Such delocalization results in a uniform distribution of charge along the Pt chain with fluctuations from site to site being $\lesssim 0.2$ electrons.

We thank Dr. G. K. Wertheim for several helpful discussions.

[1]M. J. Minot and J. H. Perlstein, Phys. Rev. Letters 26, 371 (1971); H. R. Zeller, *ibid.* 28, 1452 (1972).
[2]A. N. Bloch, R. B. Wiesmann, and C. M. Varma, Phys. Rev. Letters 28, 753 (1972).
[3]K. Krogmann and H. D. Hausen, Z. Anorg. Allgem. Chem. 358, 67 (1968).
[4]W. E. Moddeman, J. R. Blackburn, G. Kumar, K. A. Mogan, M. N. Jones, and R. G. Albridge, in *Proceedings of the International Conference on Electron Spectroscopy*, 1971, edited by D. A. Shirley (North-Holland, Amsterdam, 1972), p. 725; C. D. Cook, K. Y. Wan, J. Gelius, K. Hamrin, G. Johansson, E. Olsson, H. Siegbahn, C. Nordling, and K. Siegbahn, J. Am. Chem. Soc. 93, 1904 (1971).
[5]L. A. Levy, J. Chem Soc. (London) CI, 1081 (1912).
[6]F. N. Lecrone, M. J. Minot, and J. H. Perlstein (unpublished).
[7]H. Kanter, Phys. Rev. B 1, 2357 (1970).
[8]M. A. Butler, G. K. Wertheim, D. L. Rousseau, and S. Hufner, Chem. Phys. Letters 13, 473 (1972); P. H. Citrin and T. D. Thomas, J. Chem. Phys. 57, 4446 (1972).
[9]D. L. Rousseau and M. A. Butler (unpublished).
[10]L. V. Interrante and F. P. Bundy, Inorg. Chem. 10, 1169 (1971).
[11]S. Yamada, Bull. Chem. Soc. Japan 24, 125 (1951); K. Krogmann, Angew. Chem. Intern. Ed. Eng. 8, 35 (1969).

PHYSICAL REVIEW B VOLUME 7, NUMBER 1 1 JANUARY 1973

Determination of the Inelastic Scattering at Bragg Reflections of KCl by Means of the Mössbauer Effect: Contribution of Multiphonon-Scattering Terms

G. Albanese and C. Ghezzi
Istituto di Fisica dell'Università, Parma, Italy
and Gruppo Nazionale di Struttura della Materia (Consiglio Nazionale delle Ricerche)

and

A. Merlini
Physics Division, C.C.R. Euratom, Ispra, Italy

(Received 16 June 1972)

The scattering intensities of the 14.4-KeV γ rays from a Co^{57} source were measured at the {800} and {1000} reflections of KCl crystals in the temperature interval 80–900 °K. The elastic and inelastic components of the scattered intensities were separated by means of nuclear-resonance absorption. The temperature dependence of the inelastic intensities was in satisfactory agreement with the calculated one, when the contributions of multiphonon scattering terms were included in the evaluation of the thermal diffuse-scattering intensity. The Debye temperature $\Theta = 230 \pm 4$ °K which was derived from the temperature dependence of the elastic intensities was in good agreement with the value found in the literature.

I. INTRODUCTION

The high-energy resolution of the Mössbauer effect can be used to separate the thermal diffuse scattering (TDS) from the crystalline reflections. In two previous papers[1,2] we have used the 14.4-KeV ($\lambda = 0.8602$ Å) Mössbauer radiation emitted by the Fe^{57} nuclide to investigate the first-order TDS at various reflections of Si and Al crystals.

The TDS at a reciprocal-lattice point $\vec{S}/\lambda$ is composed of several contributions; each one of them corresponds to a scattering process which involves a definite number of phonons. By using the notation of James,[3] the intensity of TDS can be written

$$I\left(\frac{\vec{S}}{\lambda}\right) = |F_0|^2 e^{-2M}\left[\sum_{(\Phi j)_1} G_{(\Phi j)_1} I_0\left(\frac{\vec{S}}{\lambda} \pm \vec{g}_1\right) + \frac{1}{2!}\sum_{(\Phi j)_1}\sum_{(\Phi j)_2} G_{(\Phi j)_1} G_{(\Phi j)_2} I_0\left(\frac{\vec{S}}{\lambda} \pm \vec{g}_1 \pm \vec{g}_2\right) + \cdots \right.$$
$$\left. + \frac{1}{n!}\sum_{(\Phi j)_1}\sum_{(\Phi j)_2}\cdots\sum_{(\Phi j)_n} G_{(\Phi j)_1} G_{(\Phi j)_2}\cdots G_{(\Phi j)_n} I_0\left(\frac{\vec{S}}{\lambda} \pm \vec{g}_1 \pm \vec{g}_2 \cdots \pm \vec{g}_n\right) + \cdots\right], \quad (1)$$

where e^{-2M} is the Debye–Waller factor and I_0 is the interference function which is different from zero only when $\vec{S}/\lambda \pm \sum \vec{g}_j$ is a vector of the reciprocal lattice. The nth term inside the parentheses of (1) is the contribution to the total diffuse intensity by a process which involves the scattering by n phonons of reduced wave vectors $\vec{g}_1, \vec{g}_2, \ldots, \vec{g}_n$. Under the particular conditions of a scattering experiment, the intensity of TDS can be calculated by integrating formula (1) over a reciprocal-lattice volume τ determined by the scattering geometry (source and slit sizes and distances; scattering and crystal angles). By applying Debye's approximation, the result of the integration is, in the high-temperature limit ($kT \gg h\omega_{\Phi j}$),

$$R_\tau = |F_0|^2 e^{-2M}(A_1 T + A_2 T^2 + \cdots + A_n T^n + \cdots) , \tag{2}$$

where the coefficients $A_1, A_2, \ldots, A_n, \ldots$ contain complex geometric factors and do not depend on temperature. If the volume τ is centered on a reciprocal-lattice node $H \equiv \{h, k, l\}$, the coefficients A_n can be written

$$A_n \sim (\sin\Theta_H/\lambda)^{2n} (1/\Theta^{2n}) , \tag{3}$$

where Θ_H is the Bragg angle and Θ is the Debye temperature of the crystal.

The multiphonon contributions to the TDS can be negligible in the case of many diffraction experiments. However, formulas (2) and (3) show that the importance of the nth contribution increases with nth power of both T/Θ^2 and the order of reflection (expressed as the sum of the squares of the reflection indices).

We have previously measured the intensity of the TDS at the Bragg peaks as a function of temperature and of the order of reflection in Si.[2] We found that the dependence of the TDS intensity on angle and on temperature was that of the one-phonon scattering term. The terms of higher than first order did not give any appreciable contribution because of the high Debye temperature (543 °K) of Si. In the present work we have applied the Mössbauer effect to study the temperature dependence of TDS at the {800} and {1000} Bragg reflections of KCl. The high order of the above reflections, the relatively low value of the Debye temperature of KCl, and the crystal temperatures are all factors which determine the presence of important contributions to the TDS by multiphonon scattering processes.

II. EXPERIMENTAL METHOD

The separation of the γ rays which are elastically scattered by the crystal from those which suffer inelastic scattering was done by using the same procedure described in previous papers.[1,2] A 100-mCi Co^{57} source (10 mm high × 5 mm wide) diffused in a chromium matrix was used together with a 310 stainless-steel absorber 98 at.% enriched in Fe^{57}, with a thickness equal to 1 mg/cm^2 of Fe^{57}. The use of a Co^{57} source in a chromium matrix and a stainless-steel absorber has the advantage that source and absorber are very close to full resonance when they are at rest.[2] The percentage of resonant absorption $P_0 = (I_\infty - I_R)/I_\infty$ on the direct beam, I_∞ and I_R being the intensities with the absorber out of and in resonance, respectively, was equal to 0.662 ± 0.03. Since this value of P_0 is high, the elastic and inelastic fractions of the radiation scattered by the crystal can be obtained with good precision.[2]

The elastic and inelastic intensities at the peaks of the {800} and {1000} reflections by KCl crystals were measured by using the reflection (Bragg) geometry in the temperature range 80–900 °K. The crystal samples intercepted all the incident beams which had a horizontal divergence of 4° at the scattering angles used in the experiment. In some cases the scattered intensities were measured as a function of the angle between the incident beam and the crystal, which was rotated around the goniometer axis (see Fig. 1); the source and the counter were set at the scattering angle $2\Theta_H$, equal to twice the Bragg angle for the reflection $H \equiv \{h, 0, 0\}$ of interest. In many cases, however, the measurements were done only at the maximum of the Bragg peak.

The crystals of KCl were rectangular lamellas (17×18 mm) about 1.2 mm thick. They were cleaved from large single-crystal ingots grown at the Institute of Physics of the University of Parma by the Kyropoulos method from superpure powders purchased from Merck. The lamellas used for the measurements were carefully selected in order to avoid those which contained large disorientations and bendings over the volume bathed by the incident beam. The criterion used for this selection was that the samples for which the Bragg peaks had an irregular shape were discarded. It was also checked that the Bragg peaks of the samples used for the measurements did retain their regular shape at the various temperatures.

The samples were mounted on a copper plate in a nitrogen atmosphere and were held vertically by thin metal springs. The copper plate was heated by a small electric furnace and the temperature was measured by a thermocouple placed on the plate. There was a temperature gradient along the direction normal to the surface of the crystal. The temperature differences between copper plate and crystal surface were measured at the various temperatures and used to correct the thermocouple readings. In this way the temperature of the crystal surface bathed by the γ-ray beam was known with a precision of ± 3 °K. For the measurements

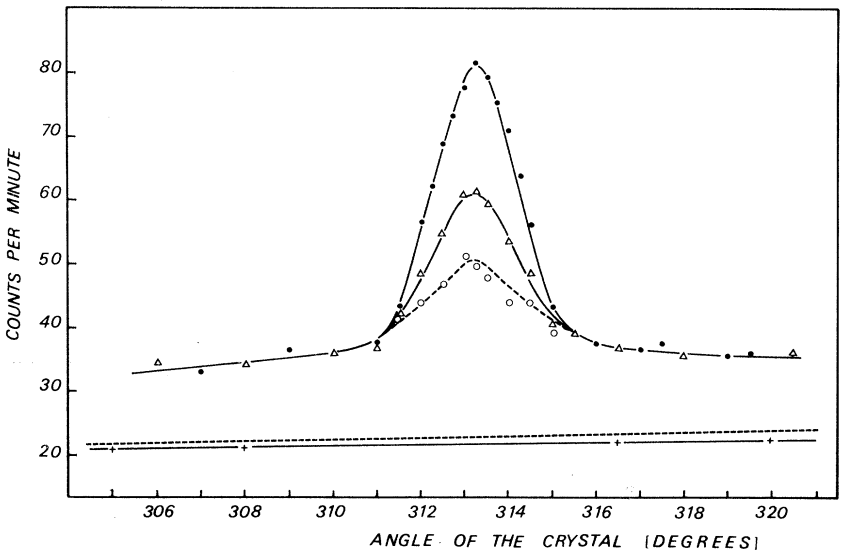

FIG. 1. Scattered intensities vs the glancing angle between incident beam and the surface of a KCl crystal, {1000} reflection, Bragg geometry, at room temperature. Filled circles and open triangles are experimental points and correspond to the curves of I_∞ and I_R (Mössbauer absorber out and in resonance, respectively). Open circles were obtained from the two above sets of experimental data and correspond to the curve (dashed) of the inelastic intensity. The straight line under the curve is the hard γ and cosmic background. The dashed straight line is the calculated Compton scattering.

below room temperature the sample was mounted in a vacuum on a metal frame, which was attached to a copper finger. This finger was cooled by a coiled tubing where liquid-nitrogen or cold-nitrogen vapors were circulated.

III. RESULTS AND DISCUSSION

Figure 1 illustrates the curves of the scattered intensities versus the angle between the incident beam and the crystal for the {1000} reflection at room temperature. The top curve is the intensity I_∞ measured with the source and the absorber out of resonance; the middle one is the intensity I_R, which was measured at resonance. The dashed curve, which has a peak at the Bragg angle, is the intensity of the inelastic scattering and was derived from I_∞ and I_R by applying Eqs. (1) of Ref. 2. The base line corresponds to the background of hard γ and cosmic radiations. The straight dashed line corresponds to the intensity of the 14.4-KeV Compton scattering, which was calculated by using a previously reported expression[1] and the values of the incoherent scattering function for K^+ and Cl^- ions given by Freeman.[4] The integrated intensity of the elastic diffraction peak was obtained by subtracting the area under the inelastic curve from the area under the curve of the total intensity I_∞. The absolute intensities of the {800} and {1000} reflections were obtained by measuring the intensity of the incident beam attenuated by cali-

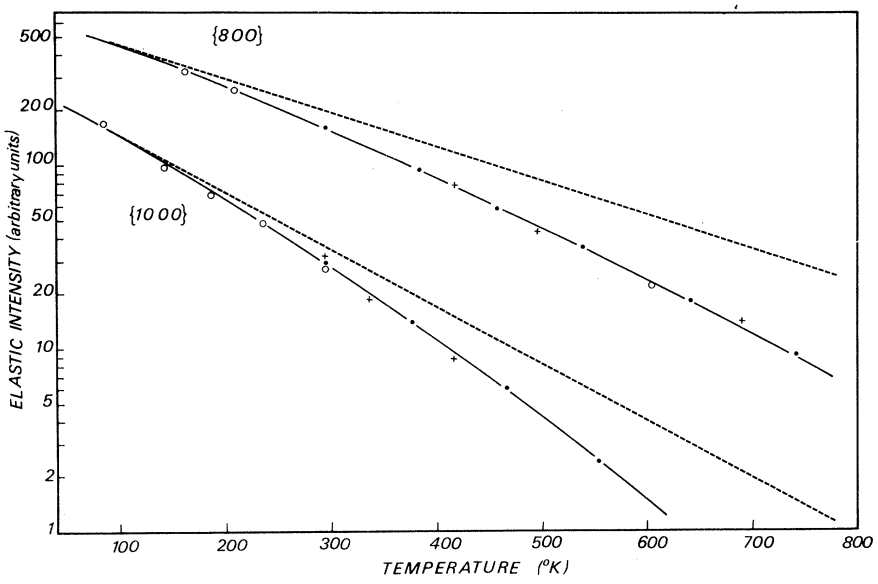

FIG. 2. Temperature dependences of the logarithms of the integrated intensities of the elastic peaks for the {800} (upper curve) and {1000} reflections (lower curve). Full circles, open circles, and small crosses are experimental points and correspond to measurements taken in different KCl samples or during different temperature cycles of the same crystal. The dashed lines are calculated by taking $\Theta = 230$ °K at every temperature. Solid lines are calculated by correcting the above value of Θ for the thermal expansion of the lattice.

brated Al filters. At room temperature these intensities were only 5% lower than those calculated for an ideally mosaic crystal when the value of the Debye temperature was taken equal to that found in the literature.[5]

A. Temperature Dependence of Integrated Intensities of Bragg Peaks

The values of the elastic intensities at the Bragg peaks are proportional to the integrated intensity of the crystal because the divergence of the incident beam in the scattering plane is considerably greater than the reflection domain of the crystal. In Fig. 2 the logarithms of the relative values of the elastic intensities at the Bragg peaks are plotted versus temperature for both the {800} and {1000} reflections. There are considerable anharmonic contributions to the Debye–Waller factor since the experimental points do not lie on a straight line. We have taken into consideration only the isotropic anharmonic correction due to the thermal expansion of the lattice. As explained by Paskin[6] the apparent Debye temperature Θ varies with temperature according to the formula

$$\Theta/\Theta_0 = [1/(1+3\beta T)]^{\gamma},$$

where Θ_0 is the Debye temperature at $T = 0\,^{\circ}\mathrm{K}$, β is the linear-expansion coefficient, and γ is the Grüneisen constant. The integrated intensities of the Bragg peaks of a mosaic crystal are proportional to a Debye–Waller factor e^{-2M_H}, where H stands for the indices of the reflection. M_H was calculated at various temperatures by taking $\Theta_0 = 230\,^{\circ}\mathrm{K}$, $\gamma = 1.60$,[7] the values of β for KCl,[8] and an average mass for the K and Cl atoms; the results are shown by the solid lines of Fig. 2. Since the two lines fit the experimental data well, it was concluded that $\Theta_0 = 230 \pm 4\,^{\circ}\mathrm{K}$, in good agreement with the value found in the literature.[5] A somewhat lower value of Θ_0 ($209\,^{\circ}\mathrm{K}$) was found by Butt and O'Connor[9] who studied the temperature dependence of the intensity of the {400} reflection by using the same experimental technique. These authors also found a strong decrease of the elastic intensity far below the line corresponding to $\Theta_0 = 209\,^{\circ}\mathrm{K}$ at about $550\,^{\circ}\mathrm{K}$; this decrease was not found in the present experiments.

B. Temperature Dependence of Inelastic Intensities at Bragg Peaks

Relative values of the inelastic intensities at the peaks of the {800} and {10 00} reflections are plotted versus temperature in Figs. 3 and 4, respectively. These curves show clearly the presence of an inversion temperature.

In order to compare the experimental values of the inelastic intensities with those predicted by the elastic wave theory of the TDS, the contributions of the one-, two-, and multiphonon terms were calculated as explained in the following.

The total TDS per atom, expressed as the sum of the contributions by the different order, can be written

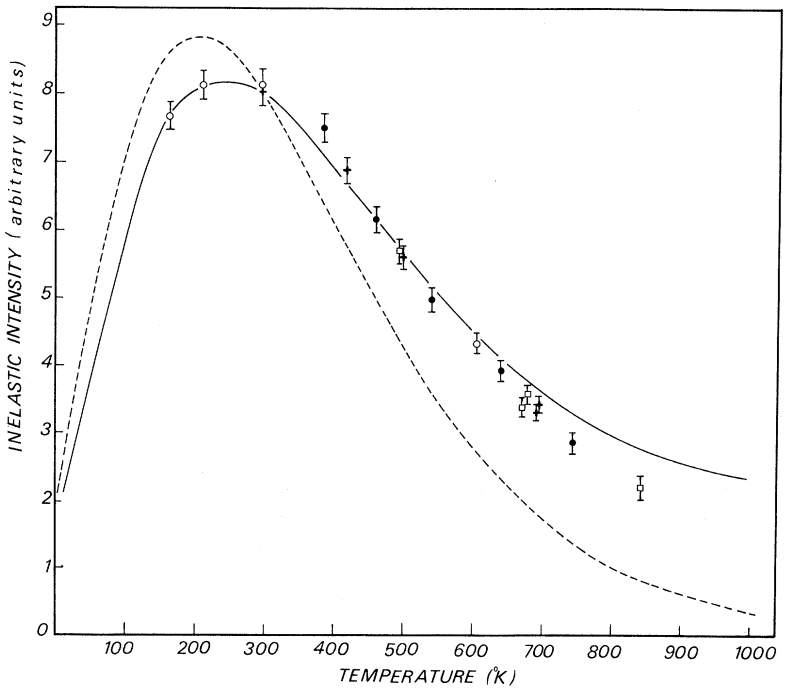

FIG. 3. Temperature dependence of the relative intensity of the inelastic scattering (TDS plus Compton) at the {800} reflection. Full and open circles, crosses, and squares are experimental points corresponding to measurements taken in different KCl samples, or during different temperature cycles of the same crystal. The dashed line was calculated by taking into account the one-phonon TDS term only, whereas the solid line includes the contributions of the first- and higher-order terms of the TDS intensity.

$$R_{\tau_H} = |F_H^0|^2 e^{-2M_H}[2M_{\tau_H} + C_2(2M_{\tau_H})^2/2! + C_3(2M_{\tau_H})^3/3! + \cdots],$$

where τ_H is a reciprocal-lattice volume determined by the geometry of the scattering experiment. If the solid is elastically isotropic and dispersion effects are negligible, the expression of the one-phonon term is

$$2M_{\tau_H} = \frac{2kT}{mN_c}\left(\frac{\sin\Theta_H}{\lambda}\right)^2 \sum_j \frac{1}{v_j^2} \times \int_{\tau_H} \frac{w(\vec{g})\cos^2(\vec{S}\cdot\vec{e}_{\vec{g}_j})}{g^2}\, d\tau , \quad (4)$$

where k, m, and N_c are the Boltzmann constant, the atomic mass, and the number of primitive unit cells per unit volume, respectively; λ and Θ_H are the wavelength of the x radiation and the Bragg angle for the reflection H; $\vec{g}_j$ is proportional to the wave vector of the phonon of polarization j; $|\vec{g}_j| = \omega_j/2\pi v_j$, ω_j and v_j being the angular frequency and the velocity of the phonon; $w(\vec{g})$ is a weight function determined by the angular distribution of the intensity of the incident beam; $\cos(\vec{S}\cdot\vec{e}_{\vec{g}_j})$ is the cosine of the angle between the scattering vector $\vec{S}$ and the unit vector $\vec{e}_{\vec{g}_j}$ in the polarization direction of the phonon $\vec{g}_j$; the sum $\sum_j$ is extended to the three polarization directions of the phonons. The approximate expression of τ_H is[2]

$$\tau_H \approx (\Delta\alpha_1 \Delta\alpha_2 \Delta\alpha_3/\lambda^3)\sin 2\Theta_H ,$$

where $\Delta\alpha_1$, $\Delta\alpha_2$ are the divergences of the incident and scattered beams in the scattering plane and $\Delta\alpha_3$ is the divergence of the scattered beam in the plane perpendicular to the scattering plane. The integral of Eq. (4) was calculated by replacing τ_H with a sphere of radius $g_m = (3\tau_H/4\pi)^{1/3}$ and $w(\vec{g})$ with a suitable function.[2] The value of this integral is approximately equal to $\pi g_m(1/v_l^2 + 2/v_t^2)$, where $v_l = 3.94\times10^5$ cm/sec and $v_t = 2.19\times10^5$ cm/sec are the longitudinal and transverse acoustic velocities of the polycrystalline solid at room temperature.[10] It was assumed that the acoustic velocities have the same dependence on temperature as the Debye temperature. The absence of dispersion effects was checked by examining the dispersion curves obtained by neutron-inelastic-scattering experiments.[11,12] Finally, the contribution of optical phonons which was calculated and added to that of Eq. (4) was found to be less than a few percent of the total one-phonon term in the whole temperature range.

The dashed curves of Figs. 3 and 4 correspond to the calculated contributions of the one-phonon scattering; these curves were normalized by taking the calculated values equal to the experimental ones at room temperature. The evident disagreement between the experimental points and the dashed curves shows that the contributions of higher-order terms are quite important.

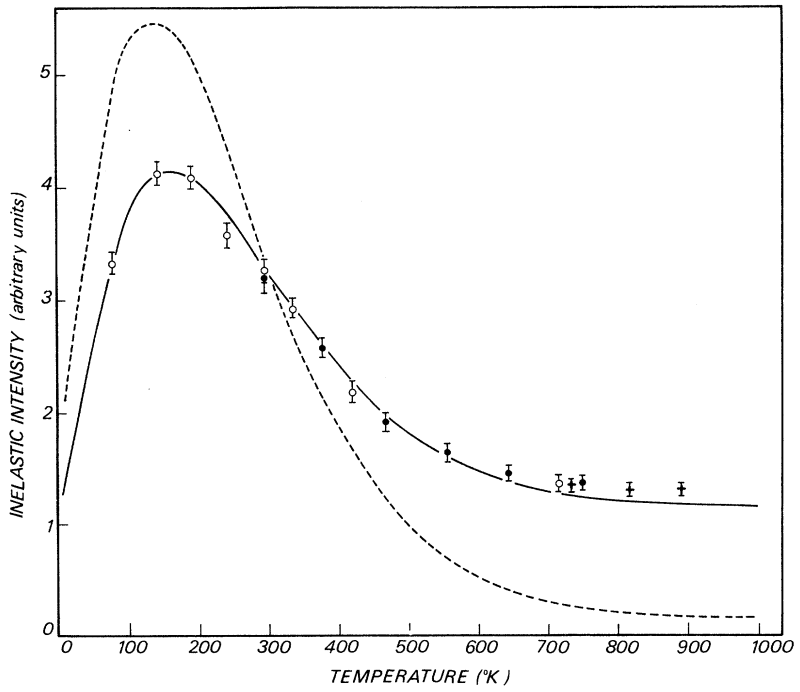

FIG. 4. Explanation is as for Fig. 3, except that the curves refer to the inelastic intensities at the {1000} reflection.

The two-phonon contribution was then calculated by using the following expression[13]:

$$\frac{C_2(2M_{\tau_H})^2}{2} = \frac{2(kT)^2}{9m^2\Omega_{BZ}}\left(\frac{\sin\Theta}{\lambda}\right)^4\left(\sum_j \frac{1}{\langle v_j^2\rangle}\right)^2 \times\sum_{hkl}\int_{\tau_H} w(\vec{g})\,d\vec{g}\int_{BZ}\frac{d\vec{g}_1}{g_1^2|\vec{g}-\vec{g}_1|^2}\,, \quad (5)$$

where, besides the symbols explained above, Ω_{BZ} is the volume of the Brillouin zone and $\langle v_j^2\rangle$ is the mean-square velocity of the elastic waves of polarization j over the Brillouin zone; $\sum_{hkl}$ is a sum over the node H and all reciprocal-lattice points which are nearest neighbors of the node H; the inside integral is extended over the entire Brillouin zone. This last integral, which was calculated by Paskin[14] and Borie,[15] is to a good approximation equal to

$$\frac{\pi^3}{g}\left[1-\frac{4}{\pi^2}\left(\frac{g}{g_{BZ}}\right)\right]\,,$$

where g_{BZ} is equal to the radius of the Brillouin zone approximated with a sphere. The contribution of the reciprocal-lattice points other than H to the sum $\sum_{hkl}$ is negligible. The sum $\sum_j(1/\langle v_j^2\rangle)$ can be calculated by using the Debye temperature $\Theta = 224\,^\circ$K (at $T = 295\,^\circ$K) of the solid:

$$\sum_j \frac{1}{\langle v_j^2\rangle} = \frac{3}{v_D^2} = 3\left(\frac{2^{1/3}hg_{BZ}}{k\Theta}\right)^2\,, \quad (6)$$

where h is the Planck constant and $v_D = 2.37\times10^5$ cm/sec, which is approximately equal to the average acoustic velocity of the polycrystalline solid $v_m = 2.49\times10^5$ cm/sec. It follows that the constant $C_2 \approx \frac{8}{9}(\frac{1}{6}\pi^2)$ in Eq. (5) when the weight function $w(\vec{g})$ is the same one used for the one-phonon scattering term. It was also checked that the value of the constant C_2 is not greatly affected by the choice of the weight function $w(\vec{g})$: $C_2 \approx \frac{1}{6}\pi^2$ when a spherically symmetric weight function was used and $C_2 \approx \frac{3}{4}(\frac{1}{6}\pi^2)$ when $w(\vec{g}) = 1$.

The contribution of terms of higher than second order was evaluated by assuming that these terms are constant inside the Brillouin zone. The validity of this assumption is discussed below with relation to the three-phonon term. We have then

$$R_{\tau_H} = R_{\tau_{H,1}} + R_{\tau_{H,2}} + (1/\Omega_{BZ}) \times(R_H - R_{H,1} - R_{H,2})\int_{\tau_H} w(\vec{g})\,d\tau\,, \quad (7)$$

where $R_{\tau_{H,1}}$ and $R_{\tau_{H,2}}$, $R_{H,1}$ and $R_{H,2}$ are the first- and second-order TDS intensity integrated over the volume τ_H and over the entire Brillouin zone, respectively. The total TDS intensity R_H integrated over the entire Brillouin zone does not depend on the choice of the model for the lattice vibrations; in fact, the integral of the total scattered intensity (Bragg plus diffuse scattering) over the Brillouin zone is not affected by the displacements of the atoms from their equilibrium positions.[16] It follows that

$$(R_H - R_{H,1} - R_{H,2}) = |F_H^0|^2 e^{-2M_H} \times\left(\frac{(2M_H)^3}{3!} + \frac{(2M_H)^4}{4!} + \cdots\right) \quad (8)$$

from the diffuse intensity expression $|F_H^0|^2 \times(1 - e^{-2M_H})$ valid for the approximation of independent vibrations of the atoms. The solid lines of Figs. 3 and 4 correspond to the total calculated TDS intensity R_{τ_H} plus the intensity of the Compton scattering; the curves were normalized to the experimental points by taking the calculated values equal to the experimental ones at room temperature. The agreement between calculated and experimental data is satisfactory. Table I summarizes the percentage contributions of first-, second, and higher-order TDS and of the Compton scattering at various temperatures for both the {800} and {1000} reflections. Table I shows clearly that the percentage contributions of multiphonon scattering terms increase rapidly with temperature.

C. Contribution of High-Order Scattering Terms to TDS

The peak of the temperature diffuse scattering at the Bragg angle becomes lower with increasing temperature until it disappears completely: Compare the curves of the {1000} reflection illustrated in Fig. 1 (the measurements were done at room temperature) with those in Fig. 5 corresponding to data taken at 716 °K. The curve of the inelastic intensity is flat and is almost independent of the crystal angle. This behavior is predicted by the

TABLE I. Contributions in percents of the first-, second-, and higher-order TDS terms and of the Compton scattering to the total inelastic intensity at the {800} and {10 00} reflections of KCl. Different contributions are calculated as explained in the text.

{hkl}	T (°K)	First order (%)	Second order (%)	Higher order (%)	Compton scattering (%)
{800}	100	91.33	5.87	0.62	2.18
	300	77.01	15.98	5.39	1.61
	700	33.53	18.64	44.26	3.57
	900	13.33	10.17	71.58	4.92
{10 00}	100	86.38	9.32	1.56	2.74
	300	61.24	21.03	14.62	3.11
	700	7.02	6.44	78.65	7.89
	900	0.92	2.43	89.29	8.64

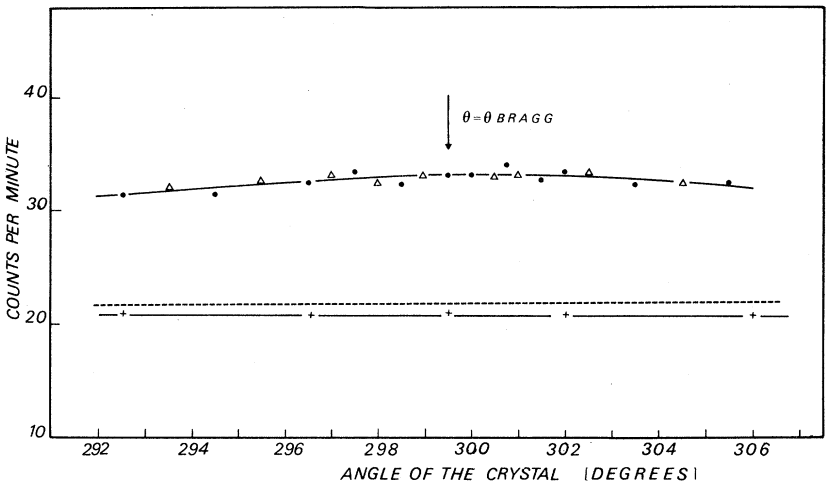

FIG. 5. Scattered intensities vs the glancing angle for the {1000} reflection at 716 °K. Explanation is as for Fig. 1. The elastic peak does not appear because its intensity is too small.

elastic wave theory of the lattice vibrations. In fact, the one-phonon term of the TDS is proportional to $1/g^2$, where g is the distance from the reciprocal-lattice node; the two-phonon term is approximately proportional to $1/g$, as shown by Eq. (5); it can be proven that the three-phonon term is proportional to $\ln(g_{BZ}/g)$ (see the Appendix). For the data of Fig. 1 the first- and second-order contributions amount to about 82% of the total inelastic intensity, whereas in Fig. 5 they amount to only 13% of the total (see Table I). The Bragg peak does not appear in Fig. 5 because its intensity is too low to be observed; this fact was checked by extrapolating the intensity of the elastic peak to the temperature (716 °K) of the measurements. A well-defined peak of the inelastic intensity is found instead for the {800} reflection at 702 °K (Fig. 6). In this case the first- and second-order contributions of the TDS amount to 52% of the total inelastic intensity (Table I), the value of $\sin\Theta_H/\lambda$ being smaller than in the case of the {10 00} reflection.

IV. SUMMARY

The intensities of the elastic and inelastic scatterings of the 14.4-KeV γ rays from a Co^{57} source were measured at the {800} and {1000} reflections of KCl crystals in the temperature range 80–900 °K. The elastic and inelastic parts of the scattered intensities were separated one from the other by using the Mössbauer effect. The most significant results are the following.

(a) The temperature dependence of the inelastic intensities differs markedly from that predicted by taking into account the one-phonon scattering contribution. A satisfactory agreement with theory

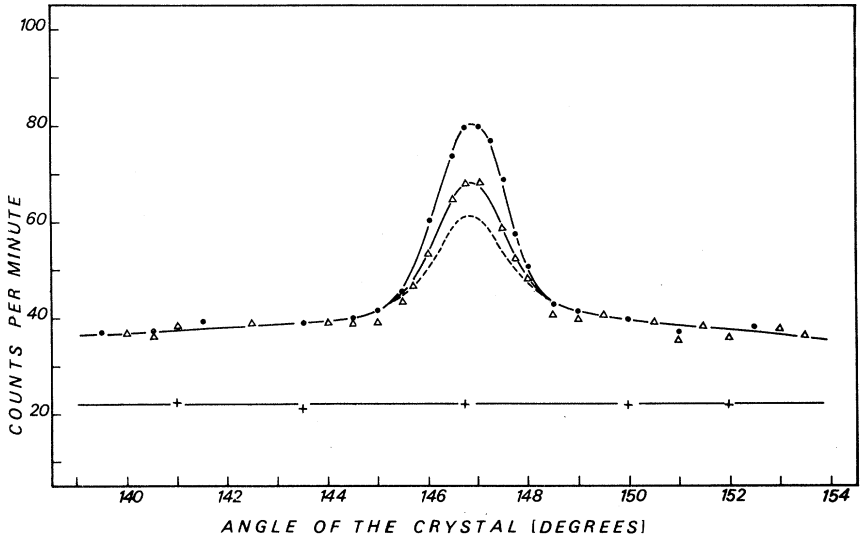

FIG. 6. Scattered intensities vs the glancing angle for the {800} reflection, at 702 °K. Explanation is as for Fig. 1.

was obtained by including the contributions of many-phonon terms in the calculation of the intensity of the thermal diffuse scattering. The two-phonon term was calculated by using the Debye model of the thermal vibrations; the contributions of higher-order terms were estimated by assuming that these terms are constant over the whole Brillouin zone.

(b) The temperature dependence of the integrated intensities of the Bragg peaks yields a Debye temperature $\Theta_0 = 230 \pm 4\,^\circ\mathrm{K}$ at $0\,^\circ\mathrm{K}$, when the effect of the thermal expansion of the lattice on Θ is considered. The above value of the Debye temperature is in very good agreement with that found in the literature.

ACKNOWLEDGMENTS

The authors are indebted to Dr. V. Stabile for his assistance during the measurements and to Professor R. Capelletti who made available the KCl single crystals.

APPENDIX

The three-phonon scattering term can be written

$$I_3\left(\frac{\vec{S}}{\lambda}\right) \sim \sum_{1,2,3} G_1 G_2 G_3 I_0\left(\frac{\vec{S}}{\lambda} \pm \vec{g}_1 \pm \vec{g}_2 \pm \vec{g}_3\right) .$$

The integration over g_3 yields

$$I_3 \sim \int \frac{d\vec{g}_1 d\vec{g}_2}{|\vec{y} - \vec{g}_1 - \vec{g}_2| \vec{g}_1^2 \vec{g}_2^2} ,$$

where $\vec{y} = \vec{g}_1 + \vec{g}_2 + \vec{g}_3$. The result of the integration over $\vec{g}_2$ is approximated by taking the first term of the series expansion[13]; it follows that

$$I_3 \sim \int \frac{d\vec{g}_2}{\vec{g}_1^2 |\vec{y} - \vec{g}_1|} = 2\pi \iint \frac{\sin\Phi \, dg_1 \, d\Phi}{(g_1^2 + y^2 - 2g_1 y \cos\Phi)^{1/2}} .$$

Since $y \ll g_{BZ}$, we find

$$I_3 \sim \ln g_{BZ}/y ,$$

where the constant terms and those proportional to y were neglected.

[1]C. Ghezzi, A. Merlini, and S. Pace, Nuovo Cimento 64B, 103 (1969).
[2]G. Albanese, C. Ghezzi, A. Merlini, and S. Pace, Phys. Rev. B 5, 1746 (1972).
[3]R. W. James, *The Optical Principles of the Diffraction of X Rays* (Bell, London, 1954), Chap. V.
[4]A. J. Freeman, Acta Cryst. 12, 929 (1959).
[5]R. W. James and G. W. Brindley, Proc. Roy. Soc. (London) 121A, 155 (1928).
[6]A. Paskin, Acta Cryst. 10, 667 (1959).
[7]C. Kittel, *Introduction to Solid State Physics* (Wiley, New York, 1966), p. 184.
[8]*American Institute of Physics Handbook* (McGraw-Hill, New York, 1963), pp. 4–73.
[9]N. M. Butt and D. A. O'Connor, Proc. Phys. Soc. (London) 90, 247 (1967).
[10]O. L. Anderson, in *Physical Acoustics*, edited by W. P. Mason (Academic, New York, 1965), Vol. III, Pt. B, p. 78.
[11]J. R. D. Copley, R. W. Macpherson, and T. Timust, Phys. Rev. 182, 965 (1969).
[12]G. Raumio and L. Almquist, Phys. Status Solidi 33, 209 (1969).
[13]B. E. Warren, *X-Ray Diffraction* (Addison-Wesley, Reading, Mass., 1968), Chap. XI, p. 165.
[14]A. Paskin, Acta Cryst. 11, 165 (1958).
[15]B. Borie, Acta Cryst. 14, 566 (1961).
[16]A. Guinier, *Théorie et Technique de la Radiocristallographie* (Dunod, Paris, 1956), Chap. XIII, p. 497.